HYPERPOLARIZATION OF ^{3}HE NUCLEI

MATEVŽ JUG

Fakulteta za matematiko in fiziko
Univerza v Ljubljani

Highly polarized ^{3}He gas is a versatile substance, with uses spanning from fundamental physics research to medical diagnostics. Two potent methods of its production, spin-exchange optical pumping and metastability-exchange optical pumping will be presented, with a focus on the first one. A slowly emerging but very promising application of polarized ^{3}He is in magnetic resonance imaging of the lungs, which will also be discussed.

HIPERPOLARIZACIJA JEDER ^{3}HE

Uporabnost močno polariziranih jeder ^{3}He sega od osnovnih raziskav v fiziki do medicinske diagnostike. V članku sta predstavljena dva učinkovita načina polarizacije plina ^{3}He, optično črpanje z izmenjavo spina in optično črpanje z izmenjavo metastabilnosti – več pozornosti je namenjene prvemu. Za konec je opisana tudi obetavna uporaba ^{3}He pri slikanju pljuč z magnetno resonanco.

1. Introduction

The nucleus of the lightest isotope of helium, ^{3}He, consists of two protons and a neutron. In its ground state, as required by the Pauli exclusion principle, the spins of the two protons point in opposite directions. The spin of the nucleus is, therefore, more or less governed by the spin of its single neutron, which gives ^{3}He some quite useful properties.

Firstly, the ^{3}He nucleus becomes a good approximation of the otherwise unstable free neutron [1]. As a scattering target, ^{3}He can be used to measure neutron form factors, providing insight into the structure of this subatomic particle. Secondly, the cross section of ^{3}He for neutron capture depends strongly on the direction of neutron's spin, making it a great spin filter (polarizer) for a beam of neutrons. Such neutron spin filters enable researchers to distinguish between nuclear and magnetic scattering in neutron scattering experiments, aiding the study of magnetic materials. They are also used for studying fundamental neutron physics, for example, asymmetries in polarized beta decay. Lastly, the large magnetic moment of ^{3}He makes it well suited for NMR experiments, such as absolute magnetometry [2] or magnetic resonance imaging of lungs [3].

All these uses require the helium gas to be polarized to levels far exceeding equilibrium polarization in any currently available static magnetic field. The angular momentum needed to achieve such a high polarization can be accumulated by the absorption of circularly polarized laser light – optical pumping of a transition that changes the magnetic quantum number by 1 ($\Delta m = 1$). Since neither the nuclear energy levels nor the electronic ground state of ^{3}He can be directly pumped in practice, two indirect optical pumping methods have been developed. *Spin-exchange optical pumping* makes use of the spontaneous exchange of spin between an alkali-metal and helium in a gas mixture, while *metastability-exchange optical pumping* bypasses the intermediary metal by pumping the atomic metastable state. Both methods use the hyperfine interaction to transfer the polarization from the atomic to the nuclear state, naming the process *hyperpolarization*.

Section 2 of this article presents the basic theory behind the first method, with a nod to currently ongoing research. The second method is touched upon briefly in section 3, mostly in comparison to the first. In the last section, interesting features of ^{3}He as a magnetic resonance imaging medium are discussed, along with a recent implementation of helium MRI.

2. Spin-exchange optical pumping

Nuclear spin polarization of a spin-1/2 substance in a magnetic field is defined as the (normalized) difference between the number of spins with magnetic quantum number $m = 1/2$ (N_+) and those with $m = -1/2$ (N_-):

$$P = \frac{N_+ - N_-}{N_+ + N_-} \,. \tag{1}$$

At sufficiently high temperatures[1], the ensemble average polarization can be approximated by

$$\langle P \rangle = \frac{\mathrm{e}^{\frac{|\gamma|\hbar B/2}{k_B T}} - \mathrm{e}^{-\frac{|\gamma|\hbar B/2}{k_B T}}}{\mathrm{e}^{\frac{|\gamma|\hbar B/2}{k_B T}} + \mathrm{e}^{-\frac{|\gamma|\hbar B/2}{k_B T}}} \approx \frac{1 + \frac{|\gamma|\hbar B}{k_B T} - 1}{1 + 1} = |\gamma| \frac{\hbar B}{2 k_B T} \,, \tag{2}$$

where γ is the gyromagnetic ratio of the nucleus, B is the external magnetic field density, T is the temperature and k_B is the Boltzmann constant [4]. This relation shows why high polarization of ^{3}He cannot be achieved simply by inserting it into a strong magnetic field. Even with its large γ, to achieve a 0.1 % polarization of room temperature (300 K) helium gas, one would need a magnetic field with a density of 400 T.

In a much more efficient approach, called spin-exchange optical pumping (SEOP), angular momentum to flip $m = -1/2$ states into $m = 1/2$ states is first transferred from circularly polarized light to vaporized alkali-metal atoms and then via the hyperfine interaction from the alkali-metal gas to helium nuclei. ^{3}He polarizations attainable this way can reach up to 88 % [1].

2.1 Optical pumping

In the first step of SEOP, laser light of appropriate wavelength and (for example) positive helicity is absorbed by the alkali-metal atom, exciting its outermost electron. The only transition allowed by the $\Delta m = +1$ selection rule is from the $m = -1/2$ ground state to the $m = 1/2$ excited state[2] (see Figure 1). Then, through collisions with other particles or through emission of a photon, the excited atom randomly relaxes into one of the two ground states. Since both ground states are being repopulated but only one of them excited, more and more atoms end up in the $m = 1/2$ state and polarization of the metal gas approaches unity.

This is of course an idealization. The most important limiting factor is the mentioned photon emission. As the gas is usually optically thick, these photons get reabsorbed and can excite the $m = 1/2$ ground state, reducing polarization. To prevent that, a small amount of N_2 buffer gas is added, so that excited metal atoms are more likely to deposit their excess energy to the many vibrational modes of nitrogen, rather than emitting it as a photon. Other noticeable sources of alkali-metal polarization loss include relaxation at the walls of the cell and loss to the rotational angular momentum of a colliding pair of atoms.

2.2 Spin exchange

When an alkali-metal atom and a helium atom collide, the directions of their spins may exchange. The (first-order) potential that a helium nucleus experiences during such a collision at a distance ξ from the metal atom is

$$V(\xi) = V_0(\xi) + \alpha(\xi)\mathbf{S}\cdot\mathbf{I} + \beta(\xi)\mathbf{S}\cdot\mathbf{N} \,. \tag{3}$$

Here, V_0 is the spin-independent part of the potential, $\mathbf{S}$ is the electron spin of the metal atom, $\mathbf{I}$ is the spin of the helium nucleus and $\mathbf{N}$ is the aforementioned relative angular momentum. The

[1] For ^{3}He, room temperature is more than enough.

[2] The quantization axis is along the laser beam. In practice, a weak homogenous magnetic field is applied in the same direction, to better define the axis and reduce relaxation effects of stray magnetic field gradients.

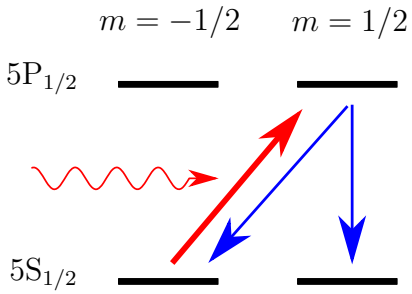

Figure 1. Relevant transitions between electron energy levels of ^{85}Rb during optical pumping. Red: photon-induced excitation with angular momentum transfer. Blue: spontaneous relaxation into any of the two ground states.

hyperfine coupling α is quite weak – the probability that a collision will result in a spin exchange is on the order of 10^{-10}.

Still, these collisions generate a steady flow of angular momentum from metal to helium gas. Under typical conditions (see next subsection), this flow and, in turn, the polarization dynamics can be modelled with a first-order differential equation

$$\frac{\mathrm{d}}{\mathrm{d}t}P = k_{SE}[A](P_A - P) - \Gamma P\,, \tag{4}$$

where k_{SE} is the spin-exchange rate coefficient, $[A]$ and P_A are the alkali-metal number density and polarization, respectively, and Γ is the relaxation rate. Taking P_A as constant (which is a good approximation, since optical pumping timescales are orders of magnitude shorter than those of spin exchange), the equation implies a maximum polarization

$$P_\infty = P_A \frac{k_{SE}[A]}{k_{SE}[A] + \Gamma} \tag{5}$$

and a time constant

$$\tau = \frac{1}{k_{SE}[A] + \Gamma}\,. \tag{6}$$

In accordance with the low probability of a spin exchange in a collision, τ is usually on the order of hours. Spin-exchange optical pumping is therefore, although very potent, relatively slow.

The relaxation rate Γ is currently poorly understood. Various measurements of τ as a function of temperature have shown that (6) can be rewritten as

$$\tau = \frac{1}{k_{SE}(1+X)[A] + \Gamma_0}\,, \tag{7}$$

meaning that a part of the relaxation rate either depends linearly on alkali-metal density, or depends on temperature similarly to $[A]$. The "X factor" of these measurements varies wildly, but shows a general dependence on surface-to-volume ratio of the cell (Figure 2), implying that most of the relaxation might come from wall collisions.

2.3 Typical experimental setup

Figure 3 shows a typical apparatus for spin-exchange optical pumping, attached to a target cell, where a scattering experiment is carried out. The spherical pumping cell is placed inside an oven that provides the necessary temperature to vaporize the alkali-metal (around 200°C). Two Helmholtz coils[3] provide a uniform magnetic field parallel to the laser beam, while the smaller coils are used to

[3]Helmholtz coils are a pair of coils on the same axis, separated by a distance equal to their radius. At the centre of such a setup, $\mathrm{d}^2B/\mathrm{d}z^2 = 0$, where z is along the axis [5].

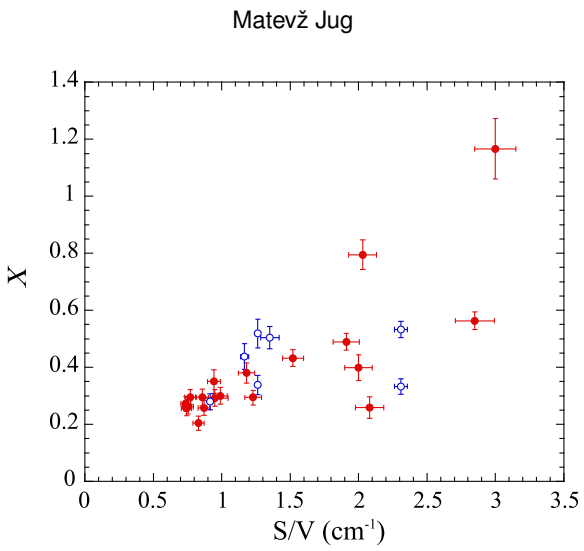

Figure 2. Measured X factors as a function of the surface-to-volume ratio for different spin-filter cells. Reproduced from [1].

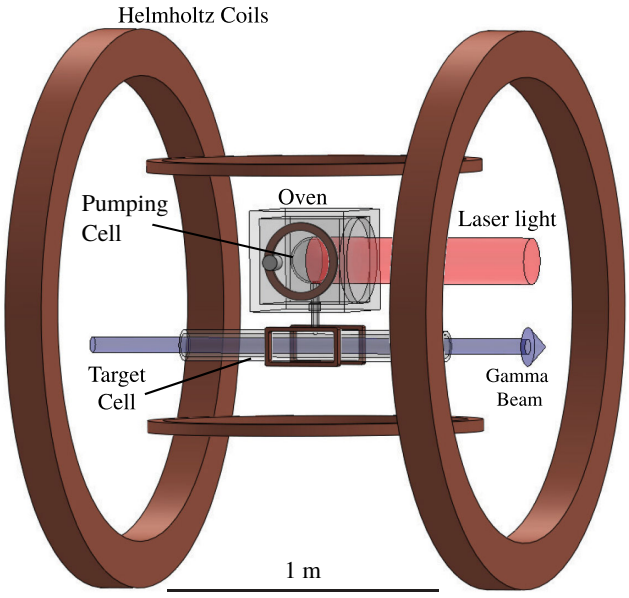

Figure 3. An example of a photon scattering experiment, employing a spin-exchange optical pumping system. Adapted from [1].

measure P and P_A. The gas mixture inside the cells usually consists of 10^{19}–$10^{20}\,\mathrm{cm}^{-3}$ of helium, $10^{14}\,\mathrm{cm}^{-3}$ of metal and $10^{18}\,\mathrm{cm}^{-3}$ of nitrogen. Alkali-metal density is fine-tuned by adjusting the temperature, as lower densities mean slower spin exchange (Eq. (4)), while higher densities require more powerful light. Typically, laser arrays with output power around 100 W are used to provide strong and spectrally narrow beams of light that cover the whole pumping cell, ensuring constant and relatively homogenous P_A despite the low diffusion rate of metal vapour.

Historically, ^{85}Rb was the alkali-metal of choice, due to the prevalence of 795 nm (rubidium) lasers. However, the undesirable spin-rotation coupling from Eq. (3) depends on the strength of the spin-orbit coupling of the metal's outermost electron, meaning that lighter metals, whose electrons have lower orbital quantum numbers, are more efficient at spin exchange. This is why, in recent years, rubidium-potassium mixtures have become popular. The optimal ratio of the two metal gasses is a setup-specific balance between spin-exchange efficiency and maximum alkali polarization (see Figure 4). In such "hybrid SEOP" systems the angular momentum is mostly transferred from light to rubidium, then to potassium and then to the helium nuclei.

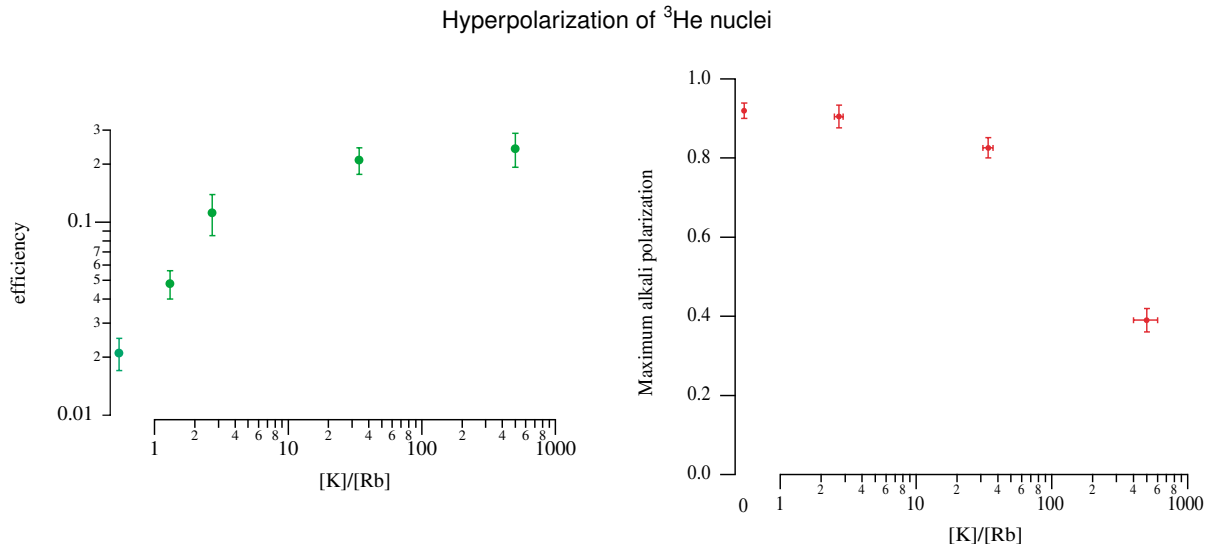

Figure 4. Dependence of spin-exchange efficiency and P_A on the ratio of the K-Rb mixture in a hybrid SEOP setup with Rb-resonant light. Spin-exchange efficiency is defined as the ratio between the rates of spin-exchange transfer to helium and alkali polarization loss. Adapted from [6].

3. An alternative: Metastability-exchange optical pumping

The first excited state of helium, the $2S_1$ state, is the longest-lived excited state of any atom [7]. Due to its longevity, this *metastable* state, denoted by He*, can be achieved simply by supplying a superfluous amount of energy to the atom[4] and letting the higher energy states decay. The transition from this state to the next excited state ($2P_0$) can be used for optical pumping similarly to the $5S_{1/2}$ – $5P_{1/2}$ transition depicted in Figure 1. As the electron and the nucleus now belong to the same atom, the hyperfine coupling between the two can then polarize the nucleus almost instantly [4]. When the excited atom collides with a ground state atom, the metastability can be exchanged, allowing the other particle to be polarized and giving rise to the term metastability-exchange optical pumping.

There is almost 100 % probability for a metastability exchange during a collision, which is many orders of magnitude larger than the probability for an SEOP spin exchange. However, to prevent collisions that are not of the type $He^* + He \longrightarrow He + He^*$ [5], the pressure of the helium gas must be sufficiently low (1–100 mbar), which slows the process of polarization down considerably. Still, MEOP remains about ten times faster than SEOP, polarizing about a bar litre of ^{3}He per hour. On the other hand, the low pressure means that for most applications a polarization-preserving compressor is needed and that continuous operation is impossible.

4. Magnetic resonance imaging with ^{3}He

Conventional MRI is a medical diagnostic technique which uses nuclear magnetic resonance of hydrogen nuclei in a strong magnetic field to produce an image. It relies on the abundance of hydrogen in human tissue, which is not a difficult condition to fulfil, since most organs are made of a large amount of water and fat. It falls short, however, at certain key organs such as lungs, which are mostly air. Due to the low equilibrium polarization (Eq. (2)) of any gas that could aid the imaging, hyperpolarization is necessary.

Apart from being relatively easy to hyperpolarize, the main reasons why ^{3}He is a great candidate for lung MRI are its long relaxation time T_1 (why this is a good thing will be clear shortly) and its

[4] This is usually done with a radio-frequency pulse [1].

[5] The two most significant of these unwanted collisions are: $He^* + He^* \longrightarrow He + He^+ + e^-$, which reduces the amount of excited atoms, and $He^* + He + He \longrightarrow He_2^* + He$, which can additionally lose some of the angular momentum to the rotational modes of the molecule.

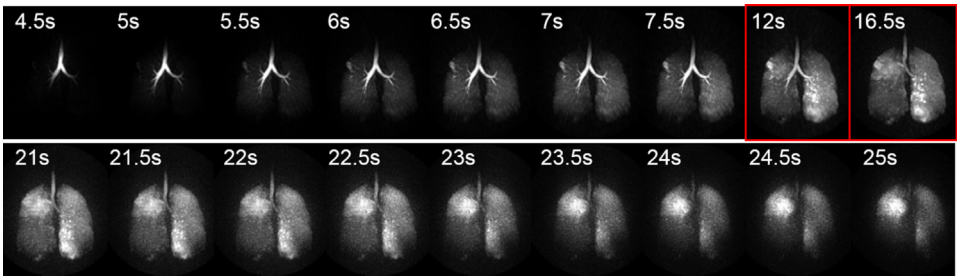

Figure 5. A series of MRI images during inhalation, breath hold and exhalation of an asthmatic patient. In the last few images, an area of trapped air is clearly visible. Reproduced from [3].

chemical inertness, meaning that the most adverse effect a patient can expect from a short exposure to ^{3}He is a temporary change in the pitch of their voice. It should be mentioned that due to the recent rise in the price of ^{3}He, the focus is actually shifting towards the other spin-1/2 noble gas, ^{129}Xe. Its properties, from polarization with SEOP to the use in MRI, are in general similar to ^{3}He and otherwise out of scope of this article.

4.1 Characteristics of ^{3}He MRI

Although the general idea is the same as in conventional MRI, the use of ^{3}He has some peculiarities that will be discussed in this section.

At the start of MRI based on ^{1}H, the polarization of hydrogen is at its equilibrium value. A typical NMR pulse sequence, such as the spin-echo sequence [8], produces a signal by destroying this polarization, which then recovers with a characteristic time T_1. In MRI involving ^{3}He, this does not happen. The initial polarization is well above the immeasurably small equilibrium value, which means that it can only decrease over time: spontaneously with T_1 and actively with each pulse. As the creation of an MRI image requires many measurements, only sequences with small flip angles ($\approx 10°$) that "use up" just a small fraction of the polarization with each pulse are feasible. On the other hand, since there is no need to wait for the polarization to recover, image acquisition can be much faster than in conventional MRI, even enabling real-time recording of the breathing cycle, such as in Figure 5.

The T_1 of helium in a patient is about 20 s [3], much less than in a specially prepared container, where it can reach up to 100 h [1]. The main contributor to this decrease are interactions with paramagnetic O_2. The relaxation rate ($1/T_1$) is directly proportional to the alveolar partial pressure of oxygen,

$$1/T_1 = k\, p_{O_2}\,, \tag{8}$$

with a coefficient, called relaxivity, of about $0.38\,\mathrm{bar}^{-1}\mathrm{s}^{-1}$ at body temperature (see Figure 6). This effect can, however, be exploited: by measuring spatial dependence of T_1, one can estimate the local consumption of oxygen.

Another disadvantage that can be turned into a feature is the high diffusivity of helium. In general, the spatial resolution of an MRI image is limited by the diffusion length $l = \sqrt{2Dt}$. For conventional MRI of protons in water and with typical observation times on the order of a millisecond, the diffusion length is about 10 µm, whereas for helium, $l \approx 930$ µm [4]. Since this is larger than the average size of an alveolus (260 µm), a diffusion-weighted image (where spins that moved farther in a set amount of time show up darker) can highlight areas of high diffusivity, indicating ruptured alveolar walls.

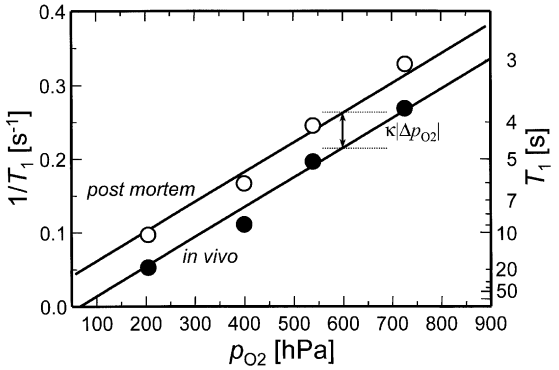

Figure 6. Relaxation time of polarized ^{3}He inside the lung of a guinea pig as a function of partial pressure of O_2 in inspired gas. As a living guinea pig absorbs oxygen, alveolar p_{O_2} is lower than the one measured, and T_1 is consequently longer. Reproduced from [4].

4.2 Example of implementation

Commercially useful implementations of MRI based on hyperpolarized gas are currently in active development. Main obstacles for SEOP-based setups are the slow speed and the toxicity of potential alkali-metal remains, whereas for MEOP-based setups, it is mostly the cumbersome application of the required specialized compressors. Alternatively, if the gas is prepared in a remote facility, there is the problem of polarization loss during transport.

An interesting system has been recently designed by researchers in Krakow [9, 10]. They have managed to compactify the MEOP apparatus so that it fits inside a typical MRI machine (Figure 7a). Using the magnetic field of the machine, they have then been able to efficiently polarize ^{3}He at a relatively high pressure of ≈30 mbar, which in turn allowed them to use a smaller pump. On the other hand, because the whole setup is inside a strong magnetic field, all the valves, as well as the motor that is driving the pump, have to be pneumatic.

After the polarization reaches the desired value, the bag that stores the hyperpolarized helium is detached and left inside the MRI machine, while the apparatus is replaced by the patient. The hyperpolarized gas therefore never leaves the homogenous magnetic field, ensuring minimal polarization loss due to stray field gradients. The bag is then connected to the patient by the ventilator setup (Figure 7b). The computer, which is connected to a system of pneumatic valves, first records the patient's natural breathing rhythm, adapts to it, releases a lungful of pure nitrogen gas to flush the lungs of oxygen, and in the next breath releases a mixture of nitrogen and helium. The patient is then instructed to hold their breath and the imaging takes place. Afterwards, the costly gas is exhaled into another bag, to be recycled.

5. Conclusion

Hyperpolarization of ^{3}He nuclei is an area of ongoing research. The lack of knowledge is most jarring when it comes to the relaxation of polarized gases, where new discoveries are expected to improve the speed of both presented methods. SEOP will most likely see additional "speed boosts" from the use of special mixtures of different alkali-metals and even more powerful lasers. Although hyperpolarized gas MRI does not yet achieve the resolution of a CT scan, its many useful characteristics provide a strong impetus for further development of this particular application. While a commercial implementation will most definitely come too late to help with our current pandemic, widespread diagnostic animations of the breathing cycle without the use of ionizing radiation may be just around the corner.

(a) The MEOP setup inside a commercial MRI machine.

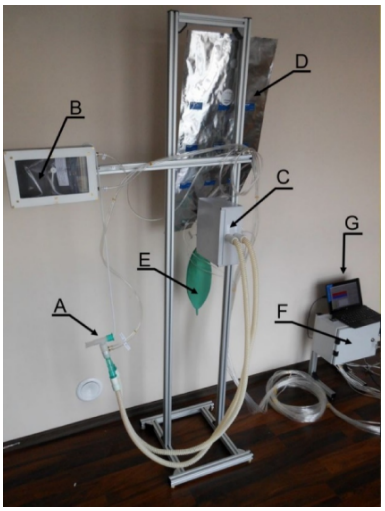

(b) The ventilator setup: **A** - mouthpiece, **B** - polarized ^{3}He bag, **C** - pneumatically controlled valves, **D** - exhaled gas collection bag, **E** - nitrogen reservoir, **F** - electronic control module, **G** - computer.

Figure 7. A system for MRI of lungs using hyperpolarized ^{3}He, described in section 4.2. Reproduced from [9] (a) and [10] (b).

References

[1] T. R. Gentile et al., Rev. Mod. Phys. **89**, 045004 (2017) https://doi.org/10.1103/revmodphys.89.045004.

[2] M. Farooq et al., Phys. Rev. Lett. **124**, 223001 (2020) https://doi.org/10.1103/physrevlett.124.223001.

[3] M. S. Albert and F. T. Hane, *Hyperpolarized and inert gas MRI* (Academic Press, 2017), https://doi.org/10.1016/C2014-0-05022-8.

[4] H. E. Möller et al., Magnetic Resonance in Medicine **47**, 10173 (2002) https://doi.org/10.1002/mrm.10173.

[5] Wikipedia contributors, *Helmholtz coil — Wikipedia, the free encyclopedia*, https://https://en.wikipedia.org/wiki/Helmholtz_coil, [accessed 30. 4. 2021].

[6] E. Babcock et al., Phys. Rev. Lett. **91**, 123003 (2003) https://doi.org/10.1103/PhysRevLett.91.123003.

[7] S. S. Hodgman et al., Phys. Rev. Lett. **103**, 053002 (2009) https://doi.org/10.1103/PhysRevLett.103.053002.

[8] T. Mertelj, "Sunkovna jedrska magnetna resonanca", in *Fizikalni praktikum V* (2016).

[9] G. Collier et al., J. Appl. Phys. **113**, 204905 (2013) https://doi.org/10.1063/1.4807836.

[10] R. Kordulasiński et al., Appl. Sci. **10**, 3163 (2020) https://doi.org/10.3390/app10093163.